Using a hybrid system to improve a lithium-ion battery in the presence of phase change material and the effect of air on the battery charge and discharge

X Zhang[1], Z Li[2], S. Mohammad Sajadi[3], Mohammed N. Ajour[4],

Nidal H. Abu-Hamdeh [5,6], Elias M. Salilih[7], A. Karimipour[8,*], Binh Nguyen Le[8]

[1] School of Electrical and Control Engineering, Xuzhou University of Technology, Xuzhou, 221018, P.R. China.

[2] Faculty of Mechanical Engineering, Opole University of Technology, 45-758 Opole, Poland.

[3] Department of Nutrition, Cihan University-Erbil, Kurdistan Region, Iraq.

[4] Center of Research Excellence in Renewable Energy and Power Systems/Energy Efficiency Group/Department of Electrical and Computer Engineering, Faculty of Engineering, King Abdulaziz University, Jeddah, Saudi Arabia.

[5] Center of Research Excellence in Renewable Energy and Power Systems/Energy Efficiency Group, King Abdulaziz University, Jeddah, Saudi Arabia.

[6] Department of Mechanical Engineering, Faculty of Engineering, K. A. CARE Energy Research and Innovation Center, King Abdulaziz University, Jeddah 21589, Saudi Arabia.

[7] Mechanical Engineering Department, Faculty of Engineering, King Abdulaziz University, Jeddah, Saudi Arabia.

[8] Institute of Research and Development, Duy Tan University, Da Nang, Vietnam

* Corresponding author

Abstract

In this article, a numerical analysis is done on the temperature of 4 plate-shaped battery cells with phase change material (PCM) chambers around each one in a rectangular shape. The batteries are placed in a channel with air flow. The study is done transiently in a time of ten minutes. The batteries are of lithium ion type and the analysis is provided in two dimensions. The battery cells are arranged in the form of two single battery cells at the beginning, and end of the channel and two battery cells in the middle of the channel. These two middle batteries are placed in parallel. By changing the distance between the two middle batteries from two to three cm, this study is conducted to investigate the temperature of each of the four battery cells and changes in the amount of frozen PCM. Finally, the results showed that the temperature of the two batteries at the beginning and the end, increased continuously during the ten minutes of the study. At a distance of three cm from the middle batteries, the lowest temperature occurred on the first and last batteries, while at the same distance, the highest temperature occurred on the middle ones. At a distance of two cm from the middle batteries, the lowest amount of frozen PCM was observed, while at a distance of three cm from the middle batteries, the highest amount of frozen PCM was found on the first and last batteries.

Keywords: Battery; Phase change material; Lithium ion; Simulation.

Nomenclature			
A_{mush}	Mushy Zone	**Greek symbols**	
Cp	Specific heat [J/(kg. K)]	β	Thermal expansion coefficient [1/K]
DOD	depth of discharge	α	Thermal diffusivity [m^2/s]
k	Thermal conductivity [W/(m. K)]	ΔH	Latent heat
h	Enthalpy	μ	Dynamic viscosity [w/(m. K)]
p	Pressure [Pa]	ρ	Density [Kg/m^3]
$\dot{q}_{ECH}$	Heat due to electrochemical reactions	φ	Phase potentials
$\dot{q}_{Short}$	Heat due to a short circuit inside the battery	σ■	effective electrical conductivity
S	Source term	ϕ■	phase potentials
t	Time		

2

T	Temperature [K]	**Subscripts**	
Re	Reynolds number	eff	Effective
Q_{Ah}	total LIB capacity	l	Liquid
j_{Short}	current transfer rate	s	Solid
j_{ECH}	volumetric current transfer rate	ref	References
u, v	Velocity components in x and y directions [m/s]	-	Negative electrode
x, y	Cartesian coordinates, [m]	+	Positive electrode
BTM	battery thermal management		
PCM	phase change material ()		

1. Introduction

Today, rechargeable batteries are widely used in many electronic devices, and it's hard to find a portable electronic device without a battery. Among these, some forms of transportation such as electric vehicles encompass both lightweight and heavy transportation means that are also dependent on batteries. The introduction of electric vehicles in recent years has raised hopes of replacing fossil fuel vehicles with these vehicles. Especially in recent years, with the advances made by Tesla, many have hoped to be able to expand electric vehicles in the world in the near future. Electric energy storage batteries are a very important part of electric vehicles. The development of this industry is highly dependent on electricity storage batteries. One of the areas in which researchers have done extensive research has been the issue of battery thermal management (BTM). BTM in hybrid vehicles is very important [1-4].

Various studies have been conducted on different methods for managing the temperature of batteries, which can be categorized into two approaches: passive and active. In active methods, battery temperature management is achieved through forced convection using a fluid by inducing mandatory flow. In this approach, external energy is required for battery cooling, but it has proven to be effective in cooling the battery. However, if there is a lack of energy available to drive the fluid circulation, this method faces challenges. This is particularly relevant as batteries have been

3

used in places where access to electrical energy has not always been available. This presents a challenge for the active battery temperature control approach. On the other hand, in passive methods, external energy is not required for battery temperature management, and phase change materials are used for controlling battery temperature. Phase change materials can store a significant amount of thermal energy within their phase transition. In this passive approach, as long as all phase change materials have not undergone phase transition, the possibility of using this method exists. The limited operational time of this method has been one of the challenges associated with its use. Continuing further, a review of some articles in the field of battery temperature management using different methods is presented. A bionic system in a cylindrical lithium battery cooling system was investigated by Yang et al. [5] Their findings demonstrated that using a bionic system over a conventional one enhances lithium battery performance. Experimental research of a cooling system for a lithium pouch battery was carried out by Li et al. [6]. The experiment was carried out using a battery thermal management system (BTMS) that was air-cooled. They showed that using a dual cooling plate improves the performance and operating conditions of the lithium-ion battery. Xu and He [7] evaluated the effect of heat loss on cooling of lithium-ion batteries and its efficiency.

Various methods have been proposed by researchers for increasing heat transfer in heat exchangers. Among these methods, the use of nanofluids, porous materials, etc. can be mentioned [8-10]. One of the methods to control the temperature of different devices is the use of PCMs. These materials, like batteries, store thermal energy. Researchers have also used PCMs in their research on batteries, etc. [11-14]. Jilte et al. [15] assessed the effect of using nanoparticles in PCMs on battery cooling. They demonstrated that the use of PCMs reduces the battery temperature to below 40 °C, leading to an increase in battery efficiency.

Considering the available technologies for cooling lithium-ion batteries, the use of hybrid systems has been highlighted as a new option. Mehrabi et al. [16] employed a hybrid system of copper foam with phase change material for the passive section and forced convection with air as the working fluid for the active section. They demonstrated that the use of the copper foam with phase change material can further reduce the battery surface temperature compared to not using it. Ranjbaran et al. [17] investigated the effect of using copper foams with different percentages on battery cooling. They found that the use of copper foam increases the thermal conductivity of the composite consisting of the phase change material and the metallic foam. However, using high-percentage metallic foam negatively affects the cooling process. In experimental studies by Zhang et al. [18], a battery cooling system was studied using a combination of expanded graphite and paraffin without an active cooling system. Their results for various operating conditions showed that this system can maintain an increase in battery temperature during charge and discharge within a safe range, but it leads to a maximum temperature difference of 5 degrees Celsius among battery cells. Although the high latent heat of paraffin melting is an important characteristic for passive cooling systems, the liquid phase of paraffin does not have efficient cooling effects and lacks the ability to control battery temperature, especially at high discharge rates. Therefore, for high-rate and long-term operations, a combination of active and passive cooling systems needs to be used to control the battery temperature increase.

Storing electrical energy in batteries causes significant advances in electrical devices, especially portable electronic devices such as laptops, mobile phones, etc. [19, 20]. Batteries have found special importance in investigations in various fields, which is also the reason why batteries are becoming more and more important [21, 22]. Batteries are also utilized in electric vehicles and many electronic devices.

Various active and passive methods have been proposed by researchers for battery temperature control. In this article, a hybrid approach incorporating both an active and a passive method has been utilized.

Due to this issue, the thermal examination of four plate battery cells is performed in this article. In an air channel, the batteries are positioned within a rectangular PCM casing. The temperature of the battery cells and the volume of frozen PCM are measured at various periods by varying the distance between the batteries. The investigation of how battery distance affects battery temperature as well as the use of PCM and airflow to control battery temperature are the novel aspects of the current work.

The focus of the article has been on the design and arrangement of lithium plate batteries in a diamond pattern, as well as the investigation of the distance between two batteries. Additionally, the utilization of both active and passive methods for battery temperature management, involving air flow and phase change materials, has been covered in the sections of the article.

2. Problem definition

Four lithium-ion plate batteries positioned in an air duct with a Reynolds number of 400 make up the geometry under study. In the channel, the battery cells are placed in three columns. The first and third columns contain a battery cell and the second one has two parallel battery cells. The distance between the two middle batteries is changed from 2 to 3 cm (Fig. 1). An enclosure filled with PCM surrounds the battery cells. The blue parts represent the PCM, the properties of which are derived from reference [23].

Air flow at a constant velocity entered the channel in a laminar flow state with a temperature of 283 Kelvin. It passed over the solid surfaces without slipping due to a no-slip condition and exited

the channel under the condition of a constant pressure, equal to the standard pressure. The initial temperature of all battery components was above 303 Kelvin, and all phase change material was initially in a molten state. The lateral walls were insulated, and the batteries were operational during the 10-minute study period.
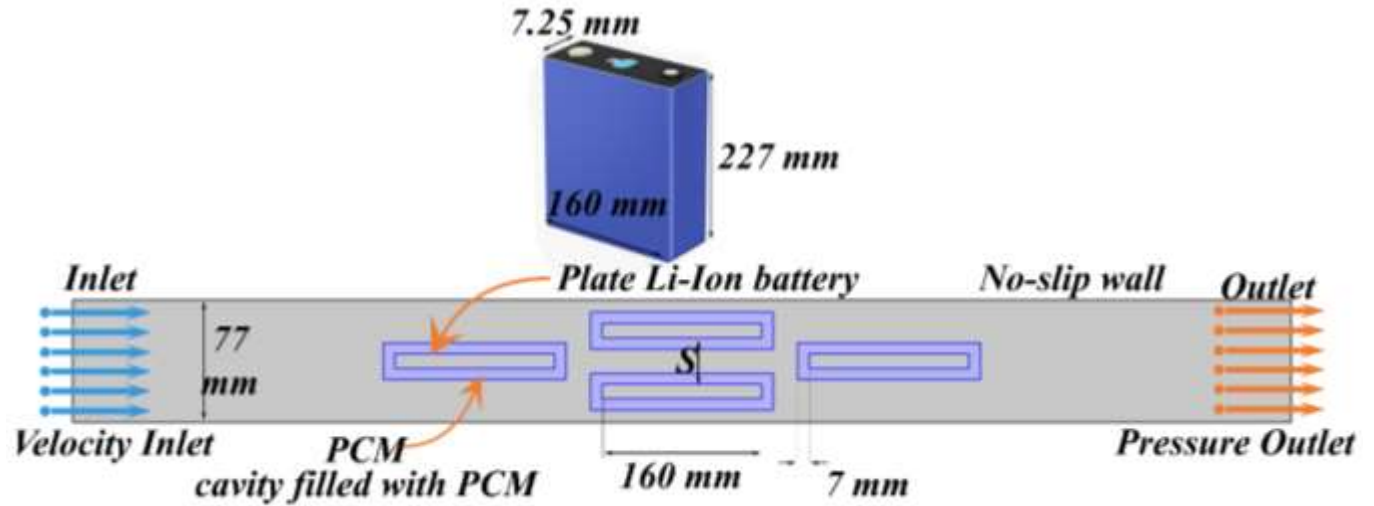

Fig. 1. Four battery cells in an air duct filled with PCM.

Table 1 presents the properties of the phase change material, while Table 2 provides the specifications of the batter.

Table 1. Thermophysical properties of PCM ($CaCl_2 6H_2O$).[23]

	melting point (°C)	C_P (J/g.K)	ρ (kg/m^3)	k (W/m.K)
$CaCl_2 6H_2O$	29.7	Solid 1.42	Solid 1680	Solid 0.626
		Fluid 2.10	Fluid 1500	Fluid 0.540

Table 2 . Lithium-ion pouch cell specifications [24]

Cathode Material	LiFePO4
Anode Material	Graphite
Electrolyte	Carbonate based
Nominal Capacity	20.0 Ah

| Nominal Voltage | 3.3 V |
| Dimensions | 7.25 mm x 160 mm x 227 mm |

3. Governing equations

Due to the performance of a lithium battery, the potential difference and resistance that occur between the electrodes result in the movement of electric current. When the battery is being charged through an external source, ion movement takes place. These chemical reactions occurring within the battery lead to the generation of heat and the production of thermal energy within the battery. The equations used to solve the battery are presented in below, which are obtained by applying Ohm's law to the electrodes and electrolytes for the electric charge [19, 25].

$$\frac{\partial(\rho C_p T)}{\partial t} - \nabla.(k\nabla T) = \sigma_+|\nabla\phi_+|^2 + \sigma_-|\nabla\phi_-|^2 + \dot{q}_{ECH} + \dot{q}_{Short} \tag{1}$$

$$\nabla.\left(\sigma_+(\nabla\phi_+)\right) = -(j_{ECH} - j_{Short}) \tag{2}$$

$$\nabla.\left(\sigma_-(\nabla\phi_-)\right) = (j_{ECH} - j_{Short}) \tag{3}$$

In the above equation, j_{ECH} can be defined as follows.

$$j_{ECH} = aY[U - (\phi_+ - \phi_-)] \tag{4}$$

The DoD value can also be calculated using the following equations.

$$DoD = \frac{Vol}{3600 Q_{Ah}}\left(\int_0^t j dt\right) \tag{5}$$

$$Y = \left(\sum_5^{n=0} a_n(DoD)^n\right) \exp\left[C_1\left(\frac{1}{T} + \frac{1}{T_{ref}}\right)\right] \tag{6}$$

$$U = \left(\sum_5^{n=0} b_n(DoD)^n\right) - C_2\left(T - T_{ref}\right) \tag{7}$$

Finally, $\dot{q}_{ECH}$ can be calculated using the following equation.

$$\dot{q}_{ECH} = j_{ECH}\left[U - (\phi_+ - \phi_-) - T\frac{dU}{dT}\right] \tag{8}$$

The equations used to solve the PCM melting and solidification fronts are also given in below. [27 ,26]. These equations include the continuity, momentum, and energy conservation equations. The buoyancy force has been considered using the Boussinesq approximation in the molten phase change material.

$$\frac{\partial}{\partial t}\rho + \nabla \cdot (\rho\vec{u}) = 0 \qquad \qquad 9$$

$$\frac{\partial}{\partial t}(\rho\vec{u}) + \nabla \cdot (\rho\vec{u}\vec{u}) = \mu\nabla^2\vec{u} - \nabla p + \rho\vec{g} + \vec{S} \qquad 10$$

$$\frac{\partial}{\partial t}(\rho H) + \nabla \cdot (\rho\vec{u}H) = \nabla \cdot (k\nabla T) \qquad 11$$

The parameter $\vec{S}$ can be defined as follows [27].

$$\vec{S} = A_{mush}\frac{(1-\gamma)^2}{\gamma^3+0.001}\vec{u} \qquad 12$$

The value of parameter γ can also be calculated at different temperatures using the following equation [27].

$$\gamma = \begin{cases} 0 & if \quad T < T_s \\ \frac{T-T_s}{T_l-T_s} & if \quad T_s < T < T_l \\ 1 & if \quad T_l > T \end{cases} \qquad 13$$

Finally, the value of enthalpy can be estimated using the following equation [27].

$$h = h_{ref} + \int_{T_{ref}}^{T} C_P \Delta T \qquad 14$$

$$\Delta H = L_h\gamma \qquad 15$$

The equations employed for steady and transient airflow, for a viscous Newtonian fluid in laminar flow, are as follows. These equations encompass the continuity, momentum, and energy conservation equations [28].

$$\frac{\partial\rho}{\partial t} + \nabla \cdot (\rho\vec{V}) = 0 \qquad 16$$

$$\frac{\partial(\vec{V})}{\partial t} + \nabla.\left(\vec{V}\vec{V}\right) = -\frac{\nabla p}{\rho} + \nabla.\left(\frac{\mu}{\rho}\left(\nabla\vec{V} + \nabla\vec{V}^T\right)\right) - \frac{(T-T_0)}{T_0}\vec{g} \qquad 17$$

$$\frac{\partial T}{\partial t} + \nabla.\left(\vec{V}T\right) = \frac{1}{\rho}\nabla.\left(k_{eff}\nabla T\right) \qquad 18$$

3.1. Numerical method and grid study

The finite element approach is used to solve the equations that control the airflow around batteries and the phase change of PCM. One of the finest possibilities for numerical solutions is to use commercial software. The equations are solved using COMSOL Multiphysics in this paper. The drawing of the geometry, meshing, solving, and extracting of the results is done using this software. Meshing is one of the most important parts of numerical simulations that must be done carefully. An unstructured grid is generated on the geometry in this paper. Table 3 displays the impact of the number of components on the battery pack's average temperature at a distance between the middle batteries of 3 cm. Based on this study, Grid 3 with 481000 elements is selected for further simulations.

Table 3. Number of elements on the average temperature of the battery pack for a distance of 3 cm between the middle batteries.

	Grid 1	Grid 2	Grid 3	Grid 4
No. of elements	181000	329000	481000	619000
Average temperature of the battery pack	304.11K	304.76K	305.08K	305.09K

Figure 2 depicts a representation of the meshing on the given geometry.
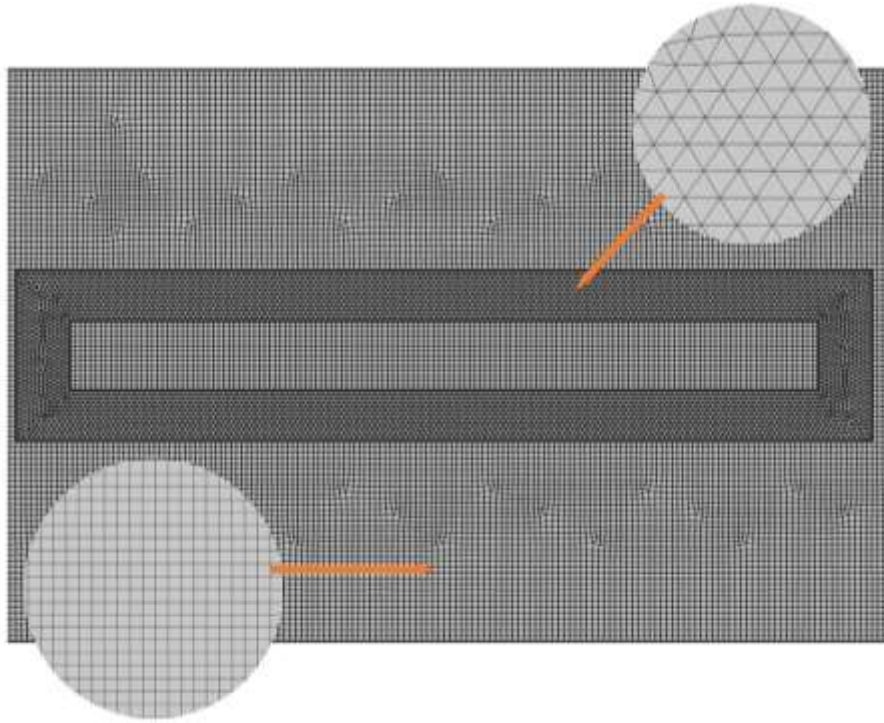
3.2. Validation

A comparison between the current findings and those of Mansir et al [29] is done in order to verify the simulations that are being used right now. The two publications compare the amounts of molten PCM at various periods and various battery lengths (Fig. 3.). The findings are in excellent accord, as can be shown. The largest difference in accuracy between the current simulations' findings and those given by Mansir et al. [29] is less than 3%, which is a reasonable amount.
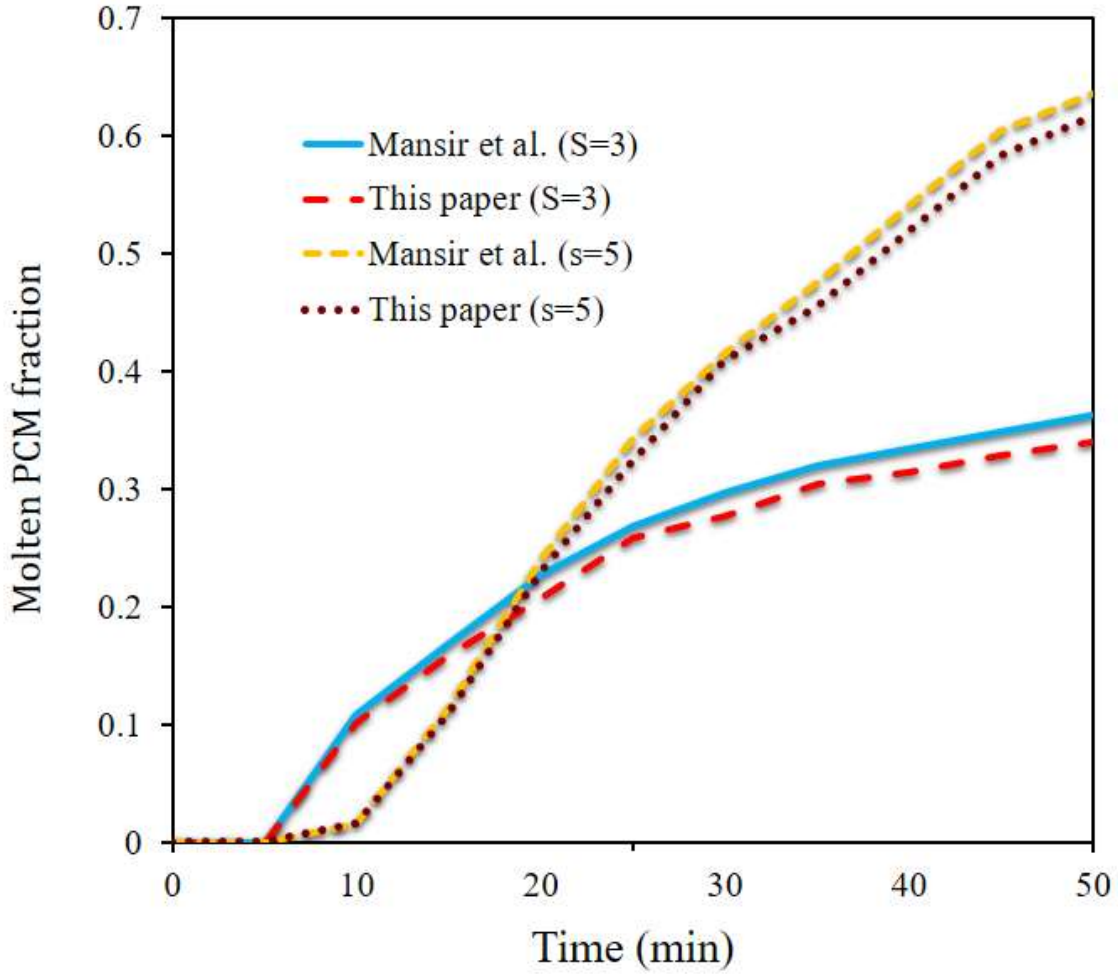
Given the significance of simulating the phase change material in this article, a validation of the PCM solution has been carried out. For this purpose, numerical and experimental data have been used for result comparison, as presented in Figure 4. This article has focused on studying the melting front of the phase change material. The volumetric fraction values of the molten phase change material at different time intervals have been compared between the current study and the work by Assis et al. [30]. According to the results, the findings of this article closely align with the experimental results, demonstrating a strong agreement.

4. Results and discussion

Fig. 5 illustrates the velocity contours for different distances of the middle batteries. The passage of air through the batteries is highly dependent on the space created between the batteries and as well as the space between the batteries and the duct wall. Where there is more space for air passage,

13

more air is passed, which makes the air velocity higher in these parts. Where there is little space, less air passes through, and as a result, the air velocity is lower. At a distance of 2 cm between the middle battery cells, the air velocity in the upper and lower parts of the batteries is slightly higher. The air velocity is considerable between the main batteries at a distance of 2.5 cm, while it is moderate near to the batteries. The air velocity is high in the center of the batteries and extremely low on each side of them at a distance of 3 cm.

Distance=2 cm

Distance=2.5 cm
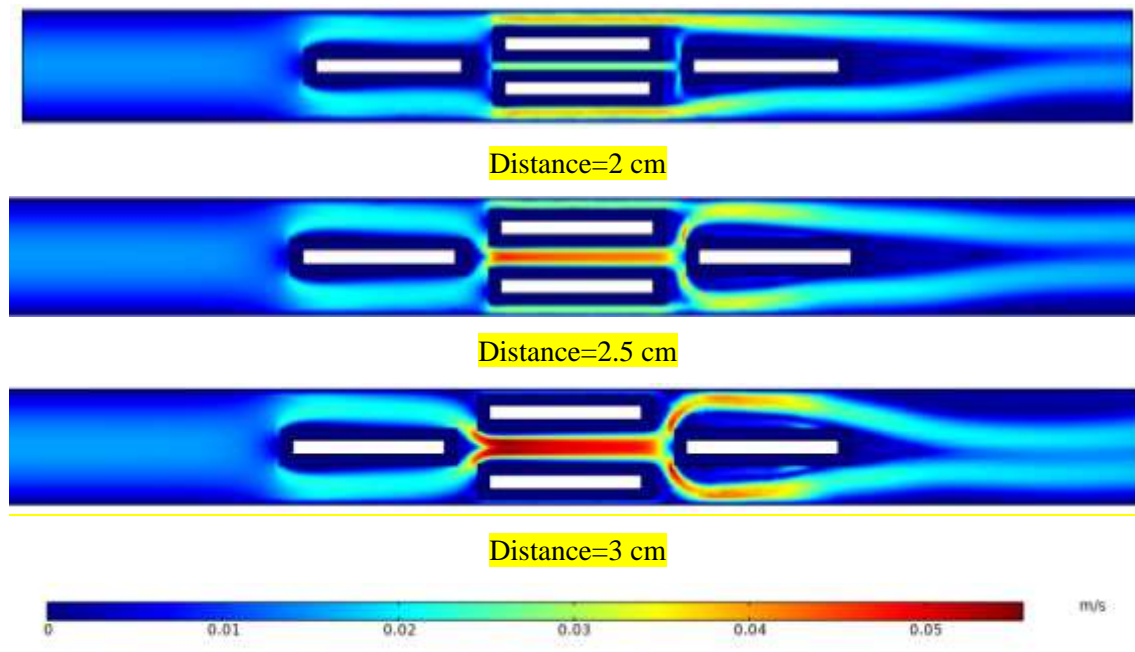
Distance=3 cm

Fig. 5. Velocity contours of the middle batteries.

Fig. 6 depicts the temperature contours for different distances of the middle batteries within 2.5, 5, 7.5, and 10 minutes. After colliding with the initial battery, the air is directed to the middle batteries, and in this part, it is directed to the wall or the middle of the two batteries due to the distance between the two batteries. After slamming against the last battery, it finally advances in

14

the direction of the outlet. The battery temperature is directly influenced by the average air velocity in each location. The battery becomes cooler as the velocity increases. The last and middle batteries' temperatures are most affected by changing the distance between them at various times. The temperature of the two center batteries decreases as the space between them increases from 2 to 2.5 cm. The last battery's temperature drops as well, although the intermediary batteries are more affected by this rise. Particularly after 10 minutes, the temperature of these two batteries lowers even further. The instantaneous temperatures of the two batteries are significantly lowered. The temperature of the intermediate batteries significantly rises when the gap between the two batteries is increased from 2.5 to 3 cm, while the temperature of the last battery falls. The final battery's temperature drops when there is 3 cm of space between the two middle batteries because more air can move through them.

In regions where there was less available space for airflow, the volume flow rate of the air passing through was lower, resulting in less effective cooling. Conversely, in areas where larger spaces were present, air easily passed through, resulting in a higher volume flow rate and better cooling in those sections. However, in some areas where the space for fluid passage was insufficient, as air reached these confined spaces, it gained velocity in order to maintain the mass conservation condition.

Distance =2 cm   Distance = 3cm

2.5 min

5 min
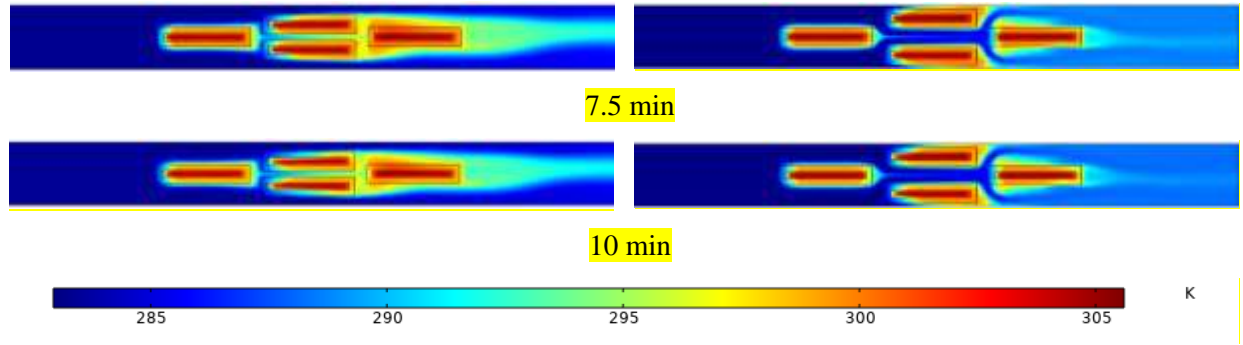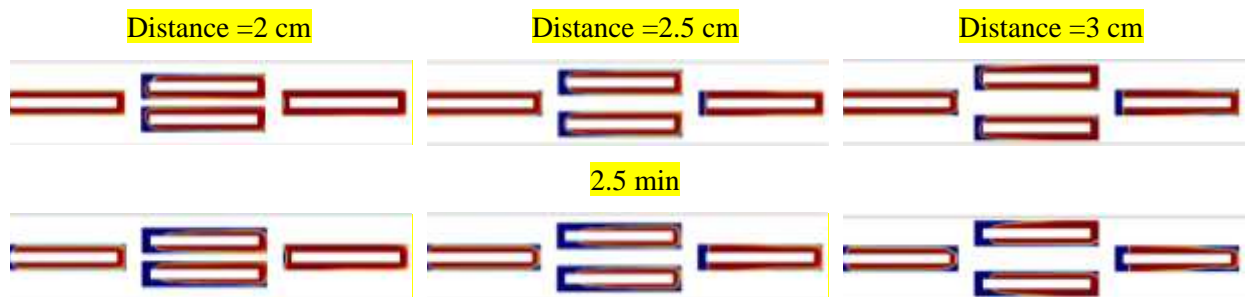
7.5 min

10 min

285   290   295   300   305   K
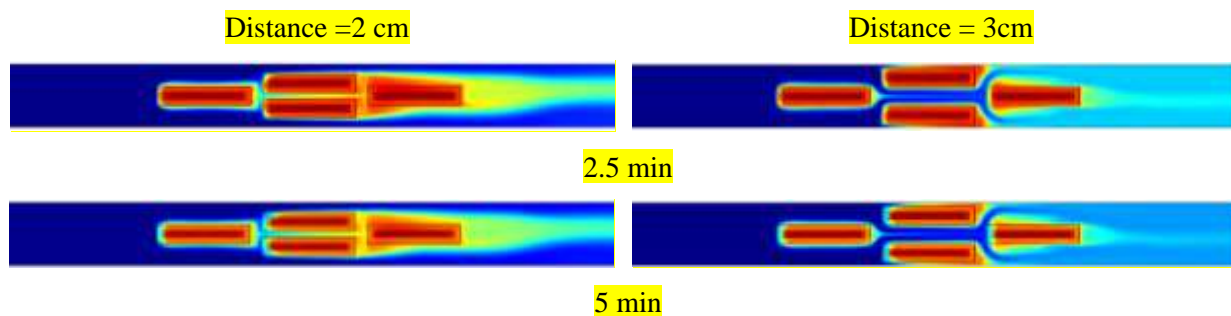
Fig. 6. Temperature contours of the middle batteries within 2.5, 5, 7.5, and 10 minutes.

Fig. 7 demonstrates the PCM volume fraction contours for different distances of middle batteries within times of 2.5, 5, 7.5, and 10 minutes. The change in velocity in each area greatly affects the rate at which the PCM solidification front is formed. At a distance of 2 cm between the middle batteries, more air passes through the sides of the batteries, so the PCM is more solidified, and the inside of the batteries has less growth in the PCM solidification front. At a distance of 2.5 cm, the solidification front has an acceptable growth in the inner and outer areas of the batteries. The strong airflow on both sides of the battery causes the growth process of the solidification front to proceed rapidly in both parts of the battery. At a distance of 3 cm, the solidification front progresses rapidly inside of the batteries and progresses slightly in the side area. The strong airflow in the middle of the batteries and the weak airflow in the side of the batteries make the solidification process in the middle of the batteries faster.
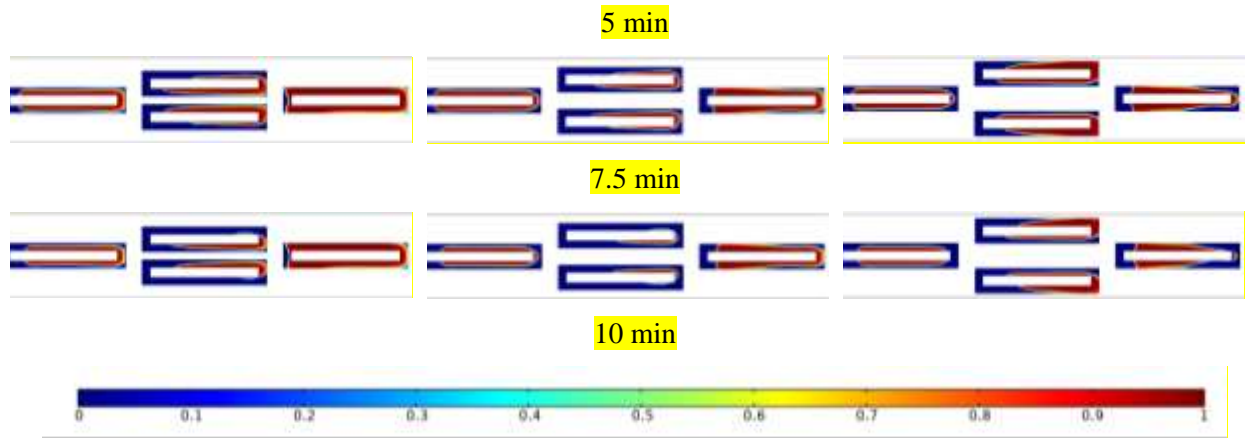
Distance =2 cm   Distance =2.5 cm   Distance =3 cm

2.5 min

16

The first battery's average temperature for up to 10 minutes is shown in Fig. 8, along with the intermediate batteries' varied distances. The first battery has the smallest alteration as a result of the altered distance between the intermediate batteries. Changes in the distance between the two middle batteries have minimal impact on the battery's average temperature because they take place behind the battery and have little impact on the air flowing through it. The temperature of this battery increases quickly in the first 10 minutes before increasing more gradually after that. But it has decreased to 305.4 degrees because of the batteries. The temperature on this battery is a small bit reduced in more than 5 minutes by more distance between the two middle batteries. The center battery benefits from improved ventilation and a minor drop in temperature when the distance between the two middle batteries is increased. By varying the distance between the two center batteries on the initial battery temperature, this little influence is not seen until the first 4 minutes. By adjusting the distance between the two middle batteries in 10 minutes, it is possible to witness the biggest change on the first battery.
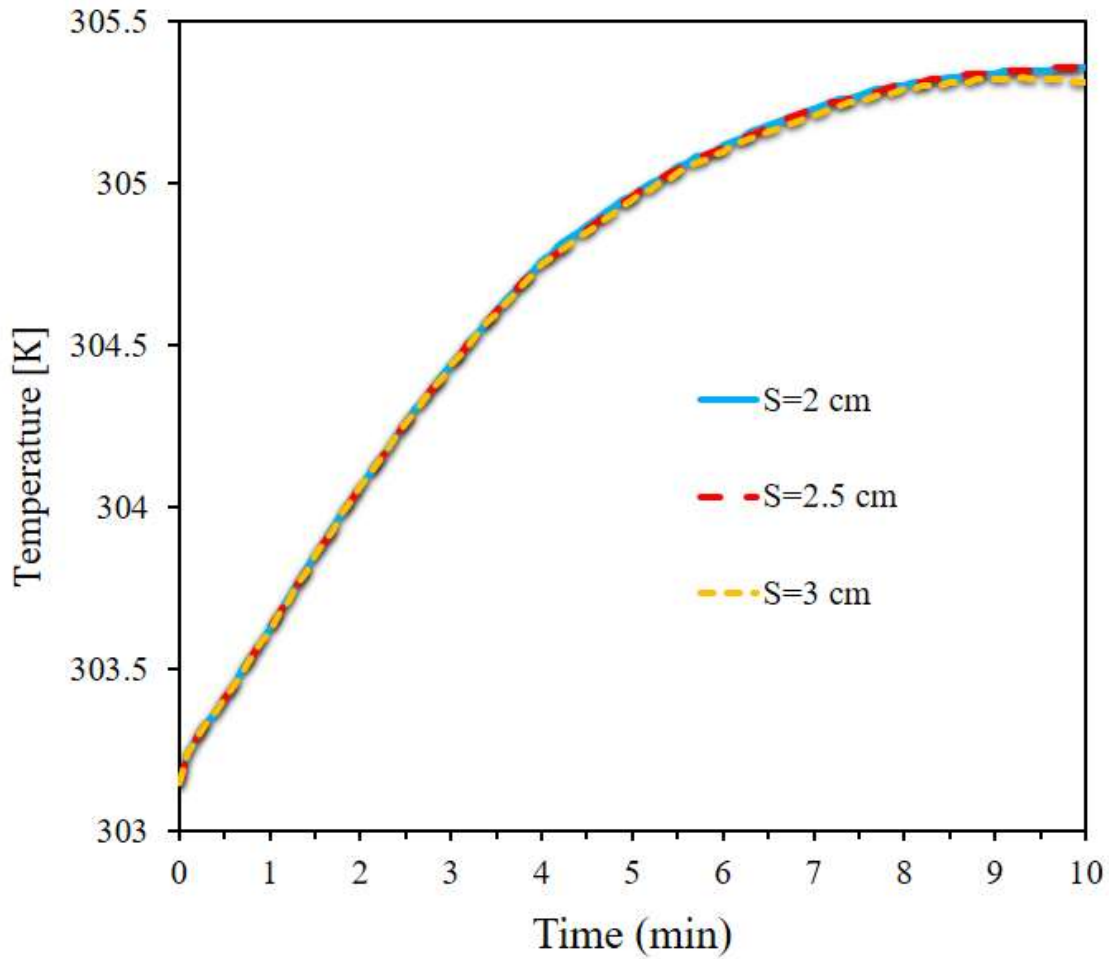
17

Fig. 8. Average temperature of the first battery for up to 10 minutes and various distances of the middle batteries.

Fig. 9 shows the average temperature of the middle batteries for up to 10 minutes for three distances between them. In general, the temperature of these two batteries is increased for 5 to 7 minutes. After this time, the temperature is decreased. Because of the distance between the two middle batteries, the times in which the battery temperature enhances are different. The maximum time that the battery temperature is improved corresponds to the distance of 3 cm. The shortest time when the battery temperature is intensified occurs when the distance between the two middle batteries is 2.5 cm. Additionally, the distance between the two center batteries affects the highest

18

temperature that the batteries may achieve. The maximum temperature difference that these two batteries reach is more than 0.5 °C for various distances between the two middle batteries. The maximum and minimum temperature increase occurs when the distance of two middle batteries is 3 cm and 2.5 cm. The amount of air flowing from each side of these two batteries is very effective on the temperature of the batteries. At a distance of 2 cm, the amount of air that passes through these two batteries is low and the amount of air that passes through the side of the duct is high. At a distance of 3 cm, the trend is reversed and a lot of air passes between the two batteries, and less air passes between these two batteries. The side where air passes more gets cooler and the side where air passes less stays warm. In these two distances of the two middle batteries, their temperature value is higher. The temperature is lower at a distance of 2.5 cm because there isn't a lot of air traveling between the two batteries and their sides, which allows for equal heat transfer from both sides and neither side.
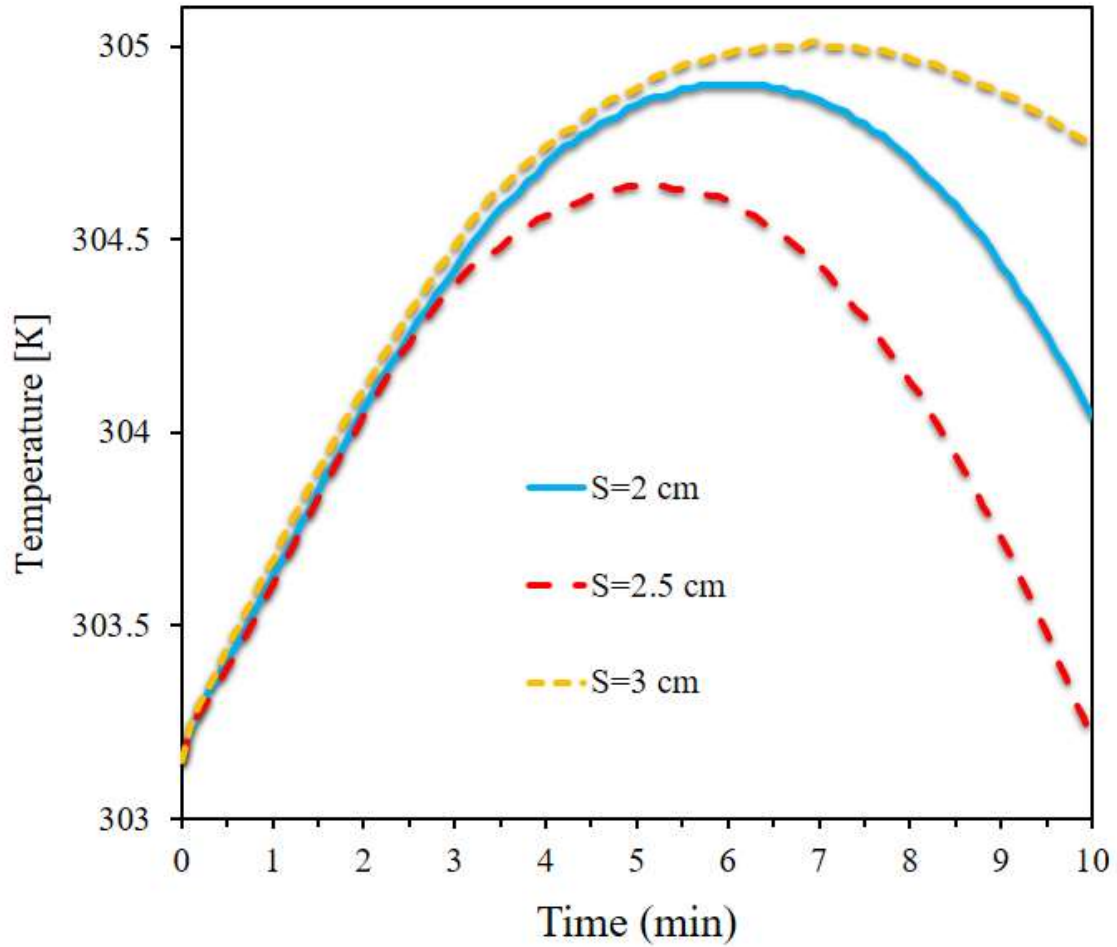
Fig. 9. Temperature of the middle batteries for up to 10 minutes for three distances among

them.

For various distances between the middle batteries, the temperature of last battery up to 10 minutes is presented in Fig. 10. When compared to the first battery, the temperature of the final battery is more sensitive to changes in the distance between the two middle batteries. This battery's temperature is constantly raised for up to 10 minutes. The difference in distance between the two center batteries causes the temperature to increase from 305.3 to 306.4. This battery has a greater pre-temperature value than the other three batteries, making it the hottest cell in the battery pack. More distance between the two middle batteries helps to lower the temperature of this battery. As

a result, the temperature of this battery is reduced by extending the distance between the two middle batteries, which is particularly noticeable over extended periods of time. More air goes between the two center batteries the more apart they are from one another. More air hits the final battery as a consequence. The air is driven up and down the batteries for a brief distance between the two main batteries. As a consequence, air flows through the top and bottom of the last cell of the battery, reducing heat transfer and raising temperature. When the gap is 3 cm, more air flows through it, cooling the final battery more effectively as a consequence of direct contact.
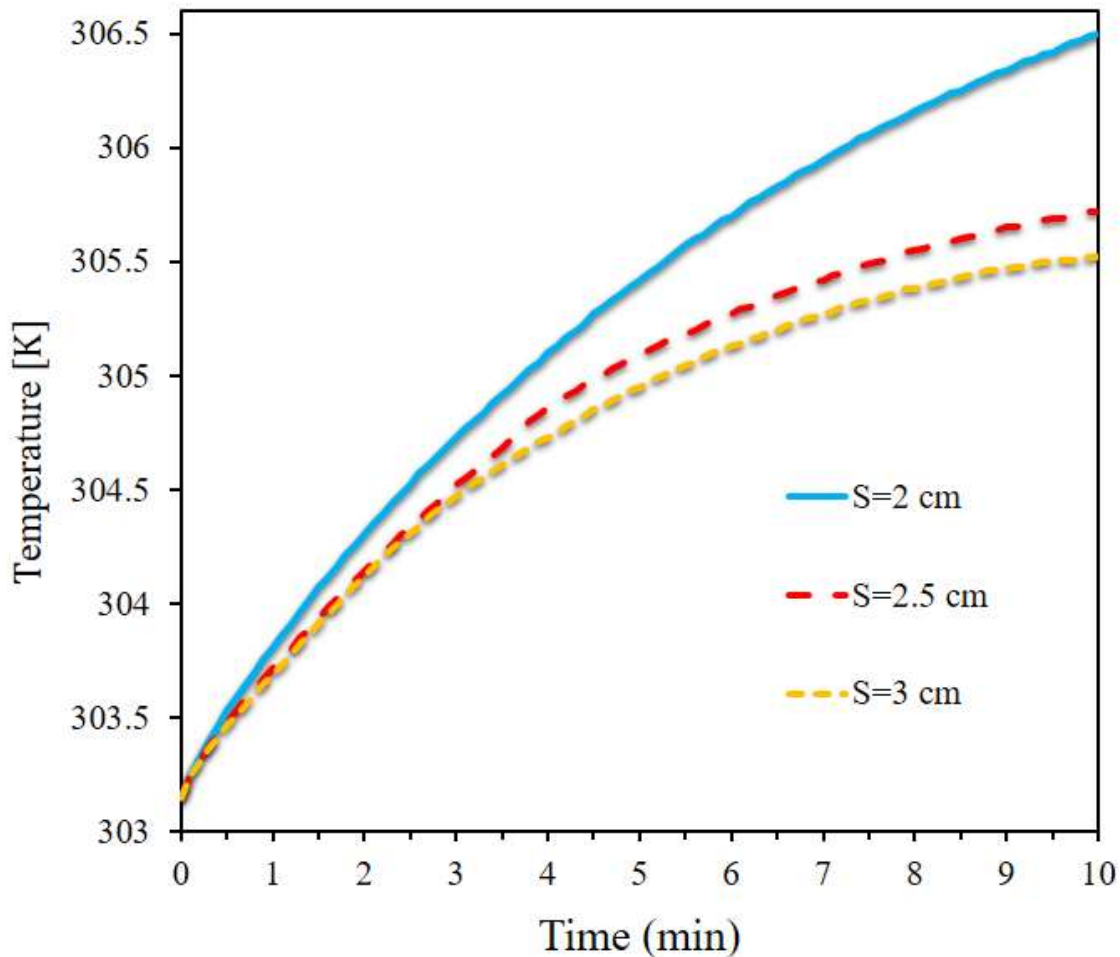
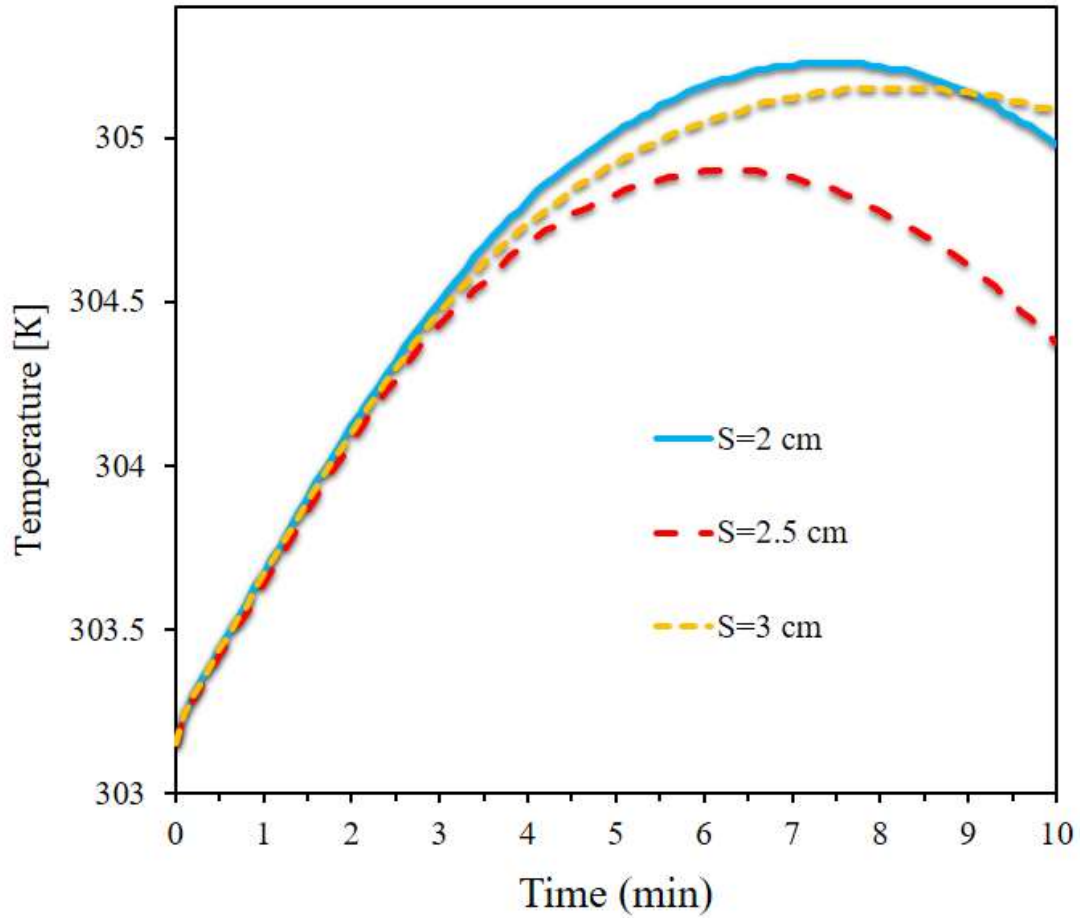Fig. 10. Average battery temperature for last battery up to 10 minutes for different distances between the middle batteries.

Fig. 11 demonstrates the average temperature of 4 battery cells for up to 10 minutes for different distances between the middle batteries. The average temperature of the battery cells is increased from 6 to 9 minutes, depending on the distance between the two middle batteries. After this time, the average temperature is reduced. Also, the average temperature reaches a maximum value depending on the distance between the two middle batteries and then reduces. When there is a 2 cm gap between the two middle batteries, the battery cells' maximum temperature occurs. The center batteries in this model have a high temperature, which raises the average temperature of the other four batteries. The distance at which there is the smallest temperature increase is 2.5 cm. The two middle batteries in this instance have low temperatures, which results in a somewhat low battery cell average temperature. The average battery temperature swings from maximum to lowest at this distance more quickly. The greatest amount of time that the battery temperature rises is connected to a 3 cm distance.

Fig. 11. Average temperature of 4 battery cells for up to 10 minutes for different distances between the middle batteries.

Fig. 12 presents the amount of frozen PCM fraction around the first battery for up to 10 minutes for different distances between the middle batteries. The amount of frozen PCM fraction around the initial battery is always decreased by up to 10 minutes. The amount of reduction and the slope of frozen PCM fraction vary according to the distance between the two middle batteries. It was found that the first battery's temperature is not significantly affected by changes in the distance between the two middle batteries. The molten PCM portion surrounding the battery, however, is significantly impacted by variations in the distance between the two middle batteries. The PCM
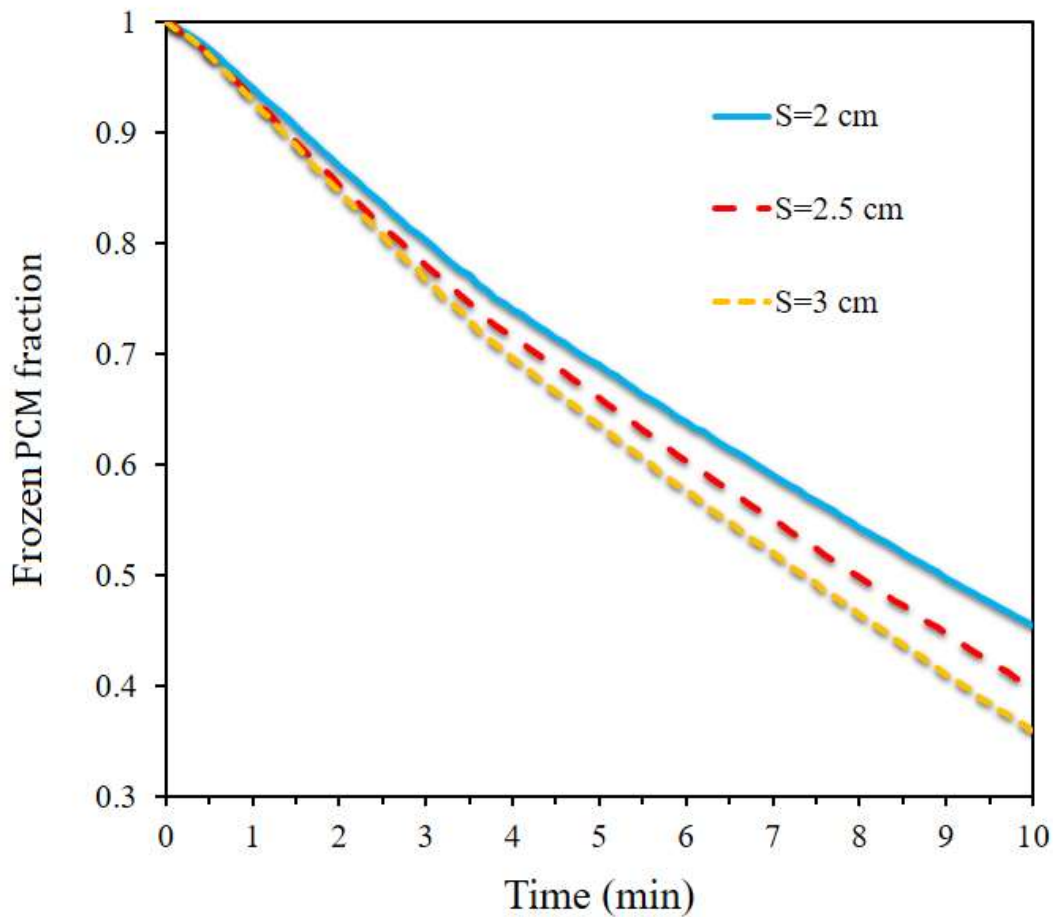
Fig. 12. Frozen PCM fraction around the first battery for up to 10 minutes for different distances between the middle batteries.

Fig. 13 illustrates the amount of frozen PCM fraction around the middle batteries for up to 10 minutes for different distances between the middle batteries. The maximum amount of phase change of PCM along with batteries is observed around the middle batteries. Depending on their distance from each other, the amount of frozen PCM fraction around these batteries changes significantly. For a distance of 3 cm, the minimum phase change happens and the lowest value of solidified PCM is observed during 10 minutes. The lowest quantity of PCM that has crystallized over time is seen at a distance of 2 cm after this. Finally, it can be shown that the largest quantity of solidified PCM is visible at various periods when the distance between the center batteries is 2.5 cm. When the distance is 2.5 cm, the PCM phase change slope is likewise greatest at various points in time. At this distance, due to the balanced passage of air through the two middle batteries and their side area, a proper solidification process occurs around both batteries. This eventually causes the amount of solidified PCM to be higher. Meanwhile, two distances of 2 and 3 cm cause the solidification process to be asymmetric and the amount of frozen PCM fraction remains high in one of the batteries due to the passage of strongly asymmetric airflow from both sides of the batteries.
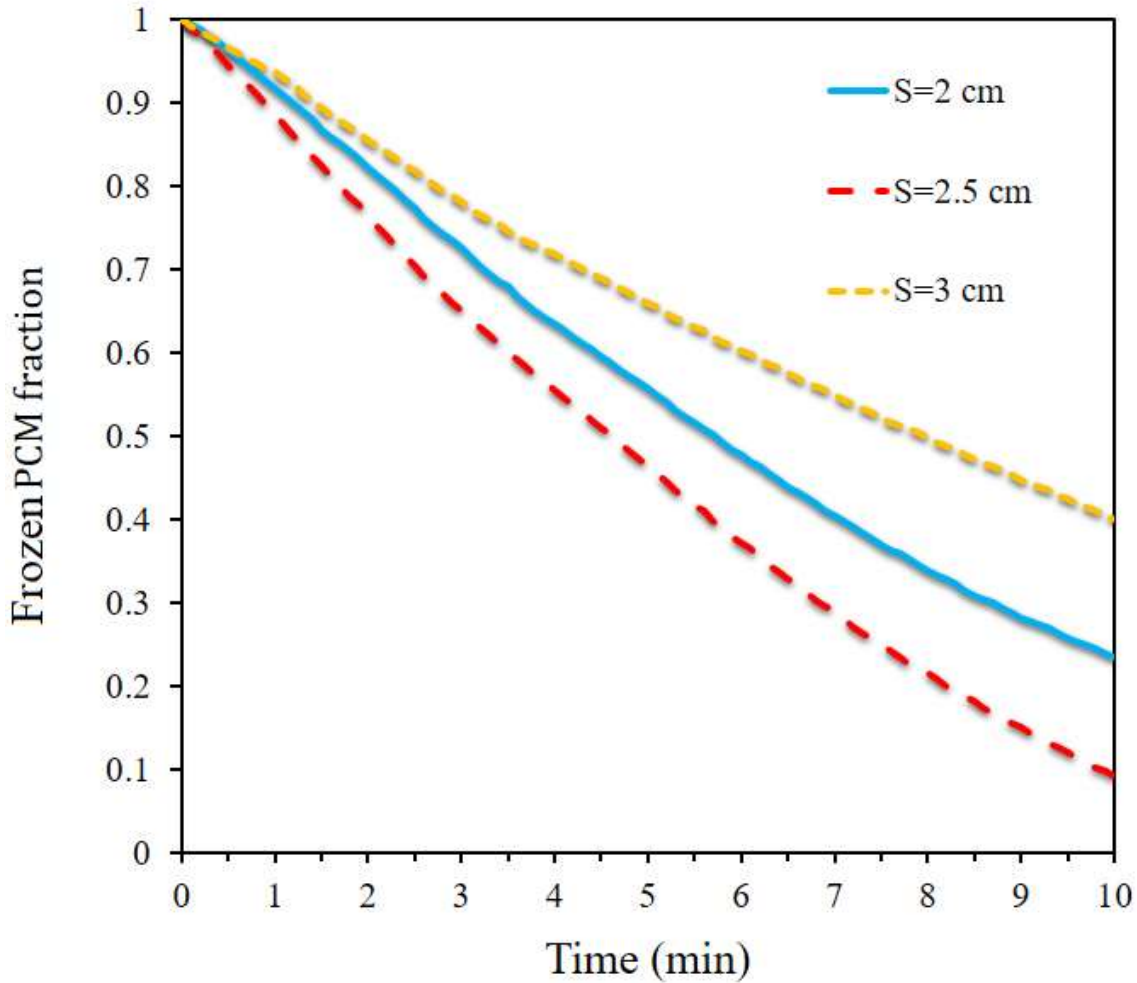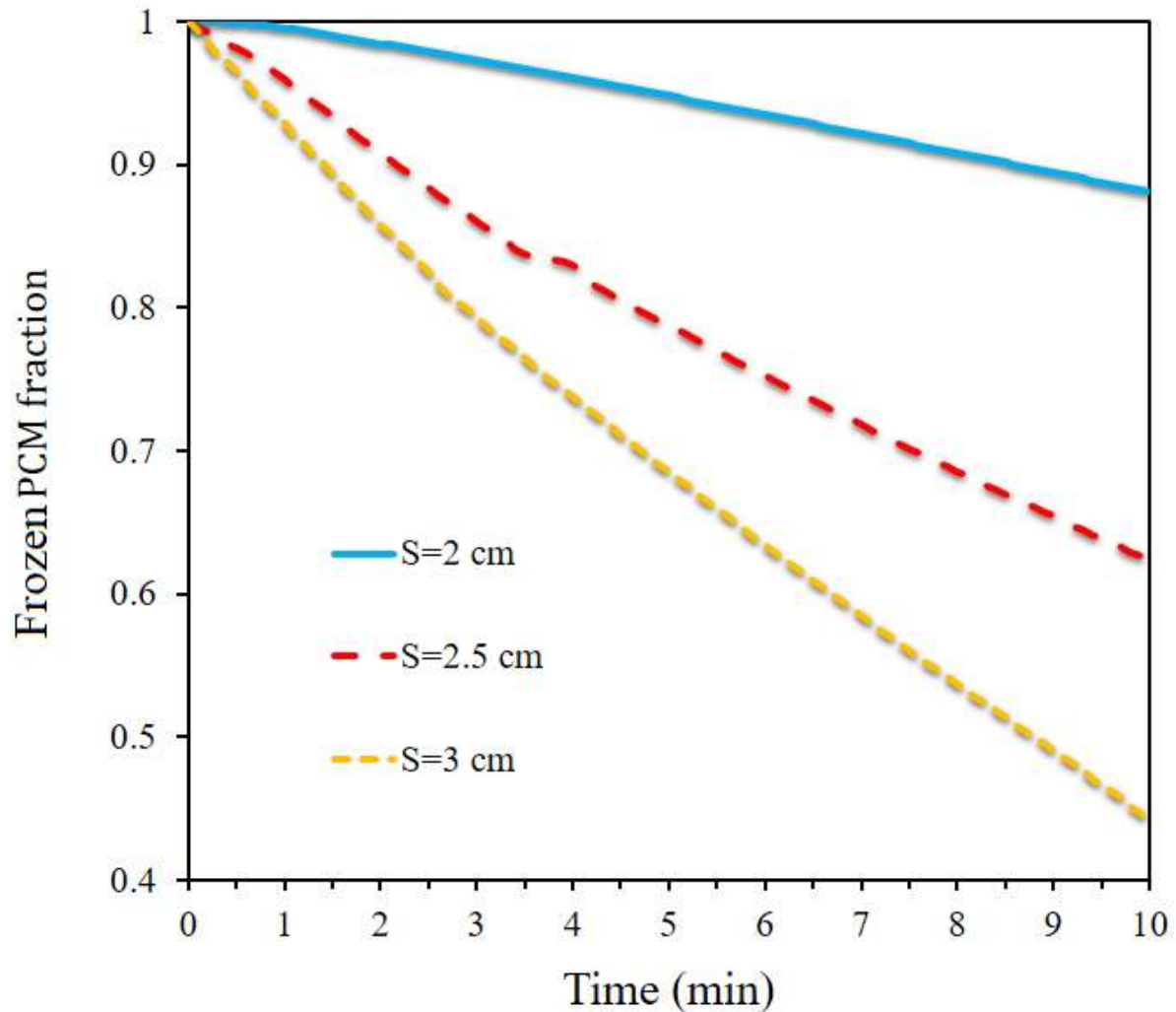
Fig. 14 depicts the amount of frozen PCM fraction around the last battery for up to 10 minutes for different distances between the middle batteries. For this battery, the maximum amount of frozen PCM is observed in 10 minutes, especially when the distance between the middle batteries is 2 cm. The amount of frozen PCM around the last battery is significantly reduced when the distance is 3 cm. For the distance of 3 cm, the highest amount of frozen PCM is observed around the last battery. The 2.5-cm distance between the middle batteries also causes the same trend between the other two distances in the PCM phase change. At a distance of 3 cm, a little more air passes through the

26

of frozen PCM fraction around the first and last batteries is reduced. However, the amount of frozen PCM around the middle batteries is not changed considerably. Finally, it can be seen that there is the maximum amount of solidified PCM at different times when the distance is 2.5 cm. The minimum amount of solidified PCM for 4 batteries corresponds to a distance of 2 cm.
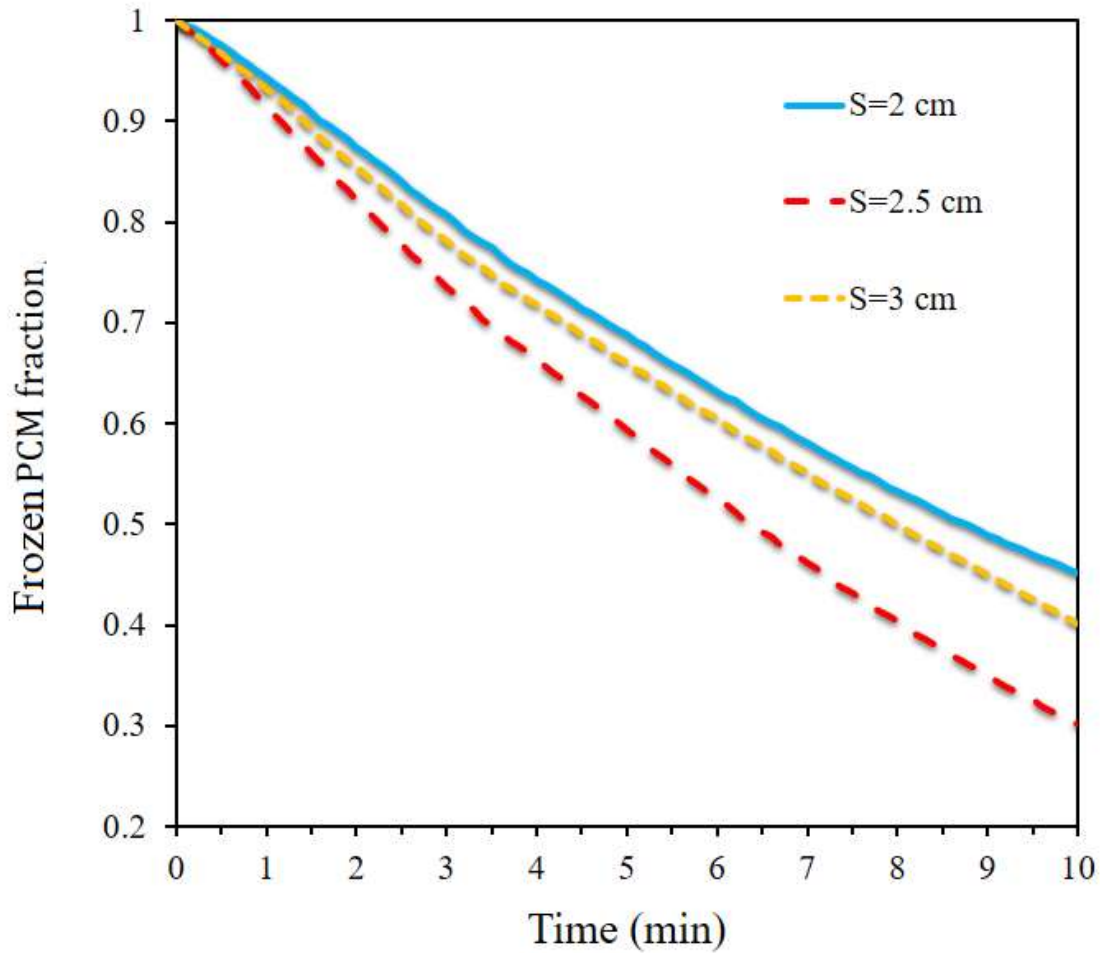

Fig. 15. Frozen PCM fraction for up to 10 minutes for different distances between the middle batteries.

5. Conclusions

This study uses numerical simulation to examine the heat transfer of four lithium-ion plate battery cells that are situated in an air duct. The battery cells are enclosed inside a container made of PCM. Two batteries are positioned parallel to each other between the first and final batteries, which are situated in the channel's midsection. The temperature of each battery cell and the quantity of frozen PCM fraction around each cell are measured by increasing the distance between the two center batteries from 2 to 3 cm, and the findings are as follows.

1- The temperature of the two first and last batteries is constantly enhanced for 10 minutes. But, the middle battery temperature first increases and then reduces after a certain time, depending on the distance between the two middle batteries.

2- The first and last batteries experience the lowest temperatures when there is a gap of 3 cm between them, whereas the intermediate batteries experience the highest temperatures at this distance. The distance of 2.5 cm results in the minimum temperature of the middle batteries.

3- The 2-cm and 3-cm distances of the middle batteries cause the minimum and maximum amount of solidified PCM, respectively, around the first and last batteries.

4- While distance among the middle batteries is 3 cm and 2.5 cm, the minimum and maximum amounts of solidified PCM occur around the middle batteries, respectively.

5- The greatest average temperature and the smallest PCM of solidified battery cells are caused by the 2-cm and 3-cm spacing of the middle batteries. The lowest temperature and the maximum quantity of PCM that has crystallized in battery cells, however, are 2.5 cm apart.

Author Declarations:

Conflicts of interest/Competing interests: There is no conflict of interest.

Availability of data and material: The data and material are available and can be presented in the case of needed.

Code availability: N/A

References

[1]T. Jin, G. Singer, K. Liang, Y. Yang, Structural batteries: Advances, challenges and perspectives, Materials today.(2022) ,

[2]O. Sadeghian, A. Moradzadeh, B. Mohammadi-Ivatloo, M. Abapour, A. Anvari-Moghaddam, J. Shiun Lim, F.P. Garcia Marquez, A comprehensive review on energy saving options and saving potential in low voltage electricity distribution networks: Building and public lighting, Sustainable Cities and Society, 72 (2021) 103064.

[3]A.V. Vykhodtsev, D. Jang, Q. Wang, W. Rosehart, H. Zareipour, A review of modelling approaches to characterize lithium-ion battery energy storage systems in techno-economic analyses of power systems, Renewable and Sustainable Energy Reviews, 166 (2022) 112584.

[4]H. Wang, S.A. Pourmousavi, W.L. Soong, X. Zhang, N. Ertugrul, Battery and energy management system for vanadium redox flow battery: A critical review and recommendations, Journal of Energy Storage, 58 (2023) 106384.

[5]W. Yang, F. Zhou, H. Zhou, Y. Liu, Thermal performance of axial air cooling system with bionic surface structure for cylindrical lithium-ion battery module, International Journal of Heat and Mass Transfer, 161 (2020) 120307.

[6]X. Li, F. He, G. Zhang, Q. Huang, D. Zhou, Experiment and simulation for pouch battery with silica cooling plates and copper mesh based air cooling thermal management system, Applied Thermal Engineering, 146 (2019) 866-880.

[7]X.M. Xu, R. He, Research on the heat dissipation performance of battery pack based on forced air cooling, Journal of Power Sources, 24.41-33 (2013) 0

[8]P. Kumar, D. Chaudhary, P. Varshney, U. Varshney, S.M. Yahya, Y. Rafat, Critical review on battery thermal management and role of nanomaterial in heat transfer enhancement for electrical vehicle application, Journal of Energy Storage.102003 (2020) 32 ,

[9]D.M. Weragoda, G. Tian, A. Burkitbayev, K.-H. Lo, T. Zhang, A comprehensive review on heat pipe based battery thermal management systems, Applied Thermal Engineering, (2023) 120070.

[10]R. Kumar, A. Mitra, T. Srinivas, Role of nano-additives in the thermal management of lithium-ion batteries: A review, Journal of Energy Storage, 48 (2022) 104059.

[11]J. Luo, D. Zou, Y. Wang, S. Wang, L. Huang, Battery thermal management systems (BTMs) based on phase change material (PCM): A comprehensive review, Chemical Engineering Journal, 430 (2022) 132741.

[12]Y. Liu, R. Zheng, J. Li, High latent heat phase change materials (PCMs) with low melting temperature for thermal management and storage of electronic devices and power batteries: Critical review, Renewable and Sustainable Energy Reviews, 168 (2022) 112783.

[13]J. Weng, Q. Huang, X. Li, G. Zhang, D. Ouyang, M. Chen, A.C.Y. Yuen, A. Li, E.W.M. Lee, W. Yang, J. Wang, X. Yang, Safety issue on PCM-based battery thermal management: Material thermal stability and system hazard mitigation, Energy Storage Materials, 53 (2022) 580-612.

[14]J. Liu, Y. Fan, Q. Xie, An experimental study on the thermal performance of mixed phase change materials-based battery cooling system, Journal of Energy Storage, 46 (2022) 103839.

[15]R. Jilte, A. Afzal, S. Panchal, A novel battery thermal management system using nano-enhanced phase change materials, Energy, 219 (2021) 119564.

[16]M. Mehrabi-Kermani, E. Houshfar, M. Ashjaee, A novel hybrid thermal management for Li-ion batteries using phase change materials embedded in copper foams combined with forced-air convection, International Journal of Thermal Sciences, 141 (2019) 47-61.

[17]Y.S. Ranjbaran, S.J. Haghparast, M. Shojaeefard, G. Molaeimanesh, Numerical evaluation of a thermal management system consisting PCM and porous metal foam for Li-ion batteries, Journal of Thermal Analysis and Calorimetry, 141 (2020) 1717-1739.

[18]J. Zhang, X. Li, F. He, J. He, Z. Zhong, G. Zhang, Experimental investigation on thermal management of electric vehicle battery module with paraffin/expanded graphite composite phase change material, International Journal of Photoenergy, 2017.(2017)

[19]W. Jiang, J. Zhao, Z. Rao, Thermal performance enhancement and prediction of narrow liquid cooling channel for battery thermal management, International Journal of Thermal Sciences, 171 (2022) 107250.

[20]Y. Zhuang, T. Chen, J. Chen, J. Li, M. Guan, Y. Chen, Thermal uniformity performance of a hybrid battery thermal management system using phase change material and cooling plates arrayed in the manner of honeycomb, Thermal Science and Engineering Progress, 26 (2021) 101094.

[21]X. Yang, Z. Zhao, Y. Liu, R. Xing, Y. Sun, Simulation of nanofluid-cooled lithium-ion battery during charging: A battery connected to a solar cell, International Journal of Mechanical Sciences, 212 (2021) 106836.

[22]S. Gungor, E. Cetkin, S. Lorente, Canopy-to-canopy liquid cooling for the thermal management of lithium-ion batteries, a constructal approach ,International Journal of Heat and Mass Transfer, 182 (2022) 121918.

[23]K. Kant, A. Shukla, A. Sharma, P. Henry Biwole, Heat transfer study of phase change materials with graphene nano particle for thermal energy storage, Solar Energy, 146 (2017) 453-463.

[24]S. Panchal, R. Khasow, I. Dincer, M. Agelin-Chaab, R. Fraser, M. Fowler, Thermal design and simulation of mini-channel cold plate for water cooled large sized prismatic lithium-ion battery, Applied Thermal Engineering, 122 (2017) 80-90.

[25]F. Chen, J. Wang, X. Yang, Topology optimization design and numerical analysis on cold plates for lithium-ion battery thermal management, International Journal of Heat and Mass Transfer, 183 (2022) 122087.

[26]A.V. Arasu, A.S. Mujumdar, Numerical study on melting of paraffin wax with Al2O3 in a square enclosure, International Communications in Heat and Mass Transfer, 39 (2012) 8-16.

[27]M.-W. Tian, G.F. Smaisim, S.-R. Yan, S.M. Sajadi, M.Z. Mahmoud, H.Ş. Aybar, A.M. Abed, Economic cost and efficiency analysis of a lithium-ion battery pack with the circular and elliptical cavities filled with phase change materials, Journal of Energy Storage, 52 (2022) 104794.

[28]M.N. Ajour, N.H. Abu-Hamdeh, O.K. Nusier, S.M. Sajadi, Developing a control program to reduce the energy consumption of nine cylindrical lithium-ion battery pack connected to a solar system by changing the distance between the batteries and the inlet and outlet of the air stream, Journal of Energy Storage, 49 (2022) 103997.

[29]I.B. Mansir, N. Sinaga, N. Farouk, U.F. Alqsair, C. Diyoke, D.D. Nguyen, Assessment of the effect of distance between lithium-ion batteries with a number of triangular blades, on the thermal management of the battery pack in a chamber full of phase change material, Journal of Energy Storage, 51 (2022) 104391.

[30]E. Assis, L. Katsman, G. Ziskind, R. Letan, Numerical and experimental study of melting in a spherical shell, International Journal of Heat and Mass Transfer, 50 (2007) 1790-1804.